^{13}C NMR, X-ray, and Differential Scanning Calorimetry Investigations of Truncated BPTI (Aprotinin) Analogues†

Poul Erik Hansen,*,‡ Wei Zhang,‡ Conni Lauritzen,‡ Søren Bjørn,§ Lars C. Petersen,§ Kjeld Norris,§ Ole Hvilsted Olsen,§ and Christian Betzel||

Department of Life Sciences and Chemistry, Roskilde University, P.O. Box 260, DK-4000 Roskilde, Denmark, Drug Discovery, NOVO-NORDISK A/S, Novo Allé, DK-2800 Bagsværd, Denmark, and Institute Physiological Chemistry, University of Hamburg, Krankenhaus Eppendorf, 20246 Hamburg, Germany

Received September 12, 1997; Revised Manuscript Received December 18, 1997

ABSTRACT: Truncated BPTI missing residues 1 and 2 is investigated together with variants thereof (Lys-15, Arg-17, and Arg-42 are replaced by other residues in various combinations). A comparison of the X-ray structure of BPTI with that of 3-58BPTI(K15R,R17A,R42S) shows only minor variations for the backbone, but the lack of salt bridge between the terminals and the lack of two N-terminal residues provide a structure open at one end. Comparisons of amide exchange rates show a dramatic increase for the most slowly exchanging NH protons of 3-58BPTI and the analogues thereof, as compared to those of the wild-type despite only small differences in the structures. The amide exchange rates for truncated analogues increase with decreasing TTEP (temperature top endothermic peak) values. On the basis of the known structural changes comparisons to ^{13}C chemical shifts are made. ^{13}C chemical shifts are assigned using the D-isotope and HMBC techniques. Excellent resolution is obtained in these 1D natural abundance spectra. ^{13}C NMR chemical shifts are shown to be able to gauge structural changes. A comparison of ^{13}C chemical shifts of WT BPTI (aprotinin) and 3-58BPTI reveals effects caused by (i) the removal of the salt bridge of the terminii, (ii) the charge of the N-terminus, and (iii) the increased mobility of the side chain of Tyr-23. Small effects are also seen due to a conformational change of the aromatic ring of Phe-4. Ring current shifts at ^{13}C chemical shifts are calculated. The difference in the calculated ring current effects are small comparing the wild-type with 3-58BPTI(K15R,R17A,R42S) provided the structures are relaxed. Protein unfolding as a function of pH and temperature is studied by DSC. Unfolding occurs at lower temperature with N-terminally truncated analogues, and the maximum is shifted toward higher pH.

Several BPTI analogues have been constructed in recent years to study specific changes in tertiary structure. X-ray (*1*−*5*) or ^{1}H NMR spectroscopy (*6*−*8*) have been used. The analogues have also been studied as folding intermediates (*9*−*11*). In addition, NMR has been applied to study the effect of salt bridge formation using BPTI analogues with modified N-terminus (*7*, *12*−*14*).

A BPTI mutant lacking the first two amino acid residues [des(Arg-1,Pro-2)BPTI] can be produced by heating or by genetic engineering (*15*). This truncated BPTI (in the following abbreviated 3-58BPTI) and other variants with specific amino acid substitutions are studied in the present work. The main focus of the investigation is the putative absence of a salt bridge between the two terminii in these BPTI derivatives. In addition, the analogues represent constructs with a broad range of thermal stabilities and a considerable variation in the total charge. Also, the number of salt bridges within the core of the protein is varied.

Amino acid substitutions by site-directed mutagenesis are generally applied to obtain information about structure and function of many proteins (*16*, *17*). This calls for convenient methods for the elucidation of structural changes induced by such specific substitutions. The structure of one of the analogues has been solved by X-ray methods. This allows a comparison between structure and the changes of the ^{13}C NMR chemical shifts. The present work tests the use of ^{13}C NMR and, in particular, the ^{13}C NMR of carbonyl resonances as a gauge of structural changes. ^{13}C NMR of proteins is gradually becoming feasable due to ^{13}C enrichment, but also due to new 2D and 3D methods, as these allow for easy assignment of the ^{13}C NMR spectra of enriched proteins (*18*). For nonenriched proteins, the HSQC (*19*) and HMBC (*20*) techniques can in principle be used. The present paper demonstrates how the isotope method (*21*) subsequently can be used in a simple fashion to assign the carbonyl region of modified proteins. ^{13}C chemical shifts are sensitive to structural changes and the variety of types of nuclei, C═O, C-α, C-*β*, etc., yield a matrix of shifts representing a very suitable and fast way to pinpoint the sites

† This work was supported by the Danish Natural Science Research Council.

* Author to whom correspondence should be addressed at Roskilde University. Phone: 45 46742432. Fax: 45 46743011. E-mail: poulerik@virgil.ruc.dk.

‡ Roskilde University.

§ Drug Discovery.

|| University of Hamburg.

[1] Abbreviations: BPTI, bovine pancreatic trypsin inhibitor; 4-BPTI, N-extended BPTI (Met-Glu-Ala-Glu-BPTI); Des(Arg-1,Pro-2)BPTI is called 3-58BPTI; DSC, differential scanning calorimetry; HMBC, heteronuclear multiple bond correlation spectroscopy; HSQC, heteronuclear single quantum correlation spectroscopy; MES, 2-[*N*-morpholino]ethanesulfonic acid; NMR, nuclear magnetic resonance; PEG, poly(ethylene glycol); T-BPTI, transaminated BPTI; TTEP, temperature top endothermic peak; WT, wild-type.

S0006-2960(97)02282-4 CCC: $15.00
Published on Web 02/27/1998

of variation in a comparison of relatively similar analogues as presented in this study. On the basis of the earlier HMBC work on WT BPTI (*22*), HMBC spectra of WT BPTI and truncated BPTI mutants have been collected to confirm the carbonyl ^{13}C assignments by the 1D isotope technique.

Ring current shifts are one of the factors which may influence ^{13}C chemical shifts (*23*). These are generally assumed to be unimportant because of the large spread in the ^{13}C chemical shifts. However, due to the fact that nuclei can come very close in proteins and also because we are comparing chemical shifts of similar residues and similar structures, ring current shifts should be considered.

Factors affecting the stability of proteins, in particular salt bridge formation, have attracted much interest (*17, 24*). Previous studies have shown that N*H* exchange rates, TTEP temperatures, and ^{1}H chemical shifts changed in a similar fashion in N-extended (*7*) and the transaminated BPTI, T-BPTI (*12*) indicating a common cause for these phenomena. In the present study, the N*H* exchange is also related to stability, and the N*H* exchange mechanism is discussed in terms of global and local unfolding (*25, 26*), just as it includes studies of effects of pH on TTEP temperatures.

EXPERIMENTAL SECTION

Analogues. Unmodified BPTI is referred to as WT BPTI or aprotinin. As it is obtained by recombinant techniques from yeast, it is free of small impurities normally found in BPTI from animal sources. The analogues, 3-58BPTI, 3-58BPTI(R42S), 3-58BPTI(R17A,R42S) and 3-58BPTI-(K15R,R17A,R42S) are obtained by similar technique and are prepared as described by Norris *et al.* (*15*).

NMR. The NMR spectra were recorded on a Bruker AC 250 instrument operating at 250 MHz for ^{1}H and at 62.89 MHz for ^{13}C. The temperature was 310 K, and the spectral resolution of the ^{1}H and ^{13}C spectra were 0.3 Hz/point. The carbonyl resonance of Glu-12 at 170.00 ppm was used as internal reference.

The concentration of proteins was normally 100−120 mg/mL (∼20 mM) in D_2O for recording of ^{13}C spectra. The spectra for observation of isotope effects were recorded at pH 2.5, whereas fully exchanged spectra were recorded at pH 2.5, 2.0, and 1.5. The effect of salt was investigated by addition of 0.3 M KCl at pH 1.5.

HMBC spectra of WT BPTI and BPTI mutants were recorded at 600 MHz ^{1}H frequency on a Varian Inova-600 spectrometer for salt free samples of 11 mM protein concentration in D_2O, pH 4.6. All the spectra were collected at 47 °C. Both the nongradient version (using phase cycling to select the required coherence transfer pathway) and the gradient version were recorded. The solvent suppression was achieved by water presaturation for the nongradient HMBC spectra, while for the gradient version, the solvent signal was well suppressed by the gradient pulses.

NH Exchange. The NH exchange rates were studied at pH 6.5 and 58 °C for WT-BPTI, 3-58BPTI, and 3-58BPTI-(R42S) and at pH 1.0 and 45 °C for 3-58BPTI, 3-58BPTI-(R42S), 3-58BPTI(R17A,R42S), and 3-58BPTI(K15R,R17A, R42S) (Tables 1 and 2). Samples contained 3−4 mM protein and, for the measurement at pH 6.5, salt was added to a concentration of 0.3 M KCl. For each sample kept at the above given temperatures, time series of 5−8 spectra were collected. The measurement was done at 250 MHz, 25 °C. Exchange rate constants were determined by an iterative least-squares fit of a first-order rate function to experimental peak heights versus time curves.

Table 1: NH Exchange Rates of Slowly Exchanging Backbone NH Protons ($\times 10^{-3}$ min^{-1})[a]

residue	3-58-BPTI	3-58BPTI-(R42S)	3-58BPTI-(R17A,-R42S)	3-58BPTI-(K15R, R17A,R42S)	WT-BPTI[b]
Ile-18	*c*	*c*	*c*	*c*	0.23
Arg-20	*c*	2.46	19.6	25.1	0.035
Tyr-21	0.30	1.97	9.66	13.2	0.008
Phe-22	0.35	2.39	12.9	17.3	0.011
Tyr-23	0.49	3.01	17.4	20.6	0.0092
Gln-31	0.56	2.92	14.8	23.4	0.060
Phe-33	*c*	1.31[d]	12.6[e]	17.0[e]	0.0038
Tyr-35	*c*	2.86[d]	12.6[e]	17.0[e]	0.200
Phe-45	0.63	4.58	18.6	28.3	0.020
Met-52	0.42	2.82	13.1	17.9	0.012
TTEP temp[f]	84	79	75	71	>100

[a] pH 1.0 and temperature = 313 K. [b] pH 0.8. Taken from ref *41*. [c] Not measured because of overlapping resonances or because the exchange was too fast. [d] The resonances of Phe-33 and Tyr-35 are completely separated and individual exchange rates are determined, but the two resonances cannot be unambiguously assigned. [e] Resonances of Phe-33 and Tyr-35 are overlapping and an average exchange rate is determined. [f] TTEP temperatures are determined at pH 5.5. Legends to figures.

Table 2: NH Exchange Rates of Slowly Exchanging Backbone NH Protons ($\times 10^{-3}$ min^{-1})[a]

residue	WT BPTI[b]	3-58BPTI	3-58BPTI(R42S)	Des(A16,R17)[c]
Ile-18	16	69		8
Arg-20	1.2[c]	114	393	5.5
Tyr-21	0.7[c]	79	342	0.083
Phe-22	0.7[c]	82	329	0.093
Tyr-23	0.7[c]	110	470	0.067
Gln-31	0.9[c]	142	491	1.1
Phe-45	3.0[c]	250	892	5.1
Met-52	75		409	

[a] pH 6.5 and temperature 331 K. [b] pH 4.6. Temperature = 309 K. Taken from ref *39*. [c] Taken from ref *7*.

DSC Experiments. Differential scanning experiments were performed on a Setaram MicroDSC (Caluire Cedex, France) with a gradient of 0.5 °C/min. Normally two cycles from 25 to 100 °C were run. Concentrations of 10 mg/mL in a 0.1 M buffer was used. All samples were filtered through a 0.22 μM filter (Millex GV) before measurements. Buffers were adjusted with HCl or NaOH. In the pH range 1−3, glycine; 4−6, sodium acetate; 5−8, sodium phosphate; 5.5 MES; 9−12, glycine were used. At pHs above 5.5, precipitation was observed during heating.

X-ray. (a) Crystallization. Crystals have been grown by vapor diffusion using the hanging drop method by Davies and Segal (*27*) up to a size of 0.5 mm × 0.3 mm × 0.7 mm. The 20 μL droplets initially contained 10 mg/mL protein in 100 mM glycine/HCl at pH 9.0 and 11% PEG. The reservoir contains 22% (w/v) PEG 4000 in 200 mM glycin/HCl. All crystals were grown at a controlled temperature of 18 °C within 5 days. They are monoclinic, space group $P2_1$, with cell dimensions $a = 29.59$ Å, $b = 41.65$ Å, $c = 41.10$ Å, and $\beta = 98.62°$. There are two molecules per asymmetric unit, with a V_m of 2.1 Å^3/Da giving a solvent content of 41% (*28*).

Table 3: Data Collection, Processing, and Refinement Details

space group	$P2_1$
cell constants	
a (Å)	29.59
b (Å)	41.65
c (Å)	41.10
β (deg)	98.62
V_m (Å^3/Da)	2.1
unique reflections	5074
resolution range	10.0−2.2
overall $R_{merge}(I)$ (%)	8.8
completeness (%)	99
final *R*-factor (%)	15.8
solvent molecules	125
deviation from ideal bond length (Å)	0.020
deviation from planar groups (Å)	0.026
deviation from chiral volumes (Å^3)	0.270
deviation of the peptide plane (deg)	4.3
mean temperature factor B (Å^2)	22.2

(b) Data Collection and Processing. For the X-ray experiments, crystals were mounted in 0.7 mm thin-walled glass capillaries. Diffraction data were collected using an image plate scanner developed in-house (Hendrix and Lentfer) (*29*) on a conventional sealed tube X-ray generator. This was operating at 50 kV and 60 mA using MoKα radiation at $\lambda = 0.71$ Å. The crystal to detector distance was set to 295 mm. A maximum resolution of 2.2 Å was reached. The crystal was rotated around *b** axis through a total of 180° with a rotatiton of 3° and an average exposure of 20 min/frame. The data were processed using a modified version of the MOSFLM package (*30*). A summary of data collection and processing is included in Table 3.

(c) Molecular Replacement. WT BPTI data (*3*) was used as model (coordinate set 6PTI from the protein data bank) in the molecular replacement for the truncated mutant. Molecular replacement was carried out applying the programs ALMN and TPSGEN of the CCP4 program suite (CCP4, 1994). The rotation function was sampled in intervals of 1.0° using all data between 10.0 and 3.0 Å. The translation parameters, restricted to the (x,z) plane, were determined using data to 2.7 Å. The solutions were clear and unambiguous in terms of both σ and in relative height showing two molecules in the asymmetric unit.

(d) Refinement. Refinement was carried out using stereochemically restrained least-squares minimization by Hendrickson and Konnert (*31*) as implemented by Baker and Dodson (*32*). The structure was refined using all reflections with no sigma cutoff. Rebuilding was carried out using the program FRODO (*33*) run on an Evans and Sutherland ESV10 interactive graphics unit. In the first stage of refinement, the low resolution data to 3.0 Å were used in 10 cycles to adjust the position of the molecues by *x,y,z* refinement. Rebuilding of the model was performed during the refinement by inspection of $2F_o - F_c$ synthesis, $F_o - F_c$ difference Fourier syntheses. Water molecules were accepted when in good electron density and reasonably H-bonded to other parts of the structure during all steps of model inspection. All waters were assigned to unit occupancy. A total of 125 molecules were located in well-defined electron density and included in the refinement.

No density could be assigned for the side chains of residues 7A and B, 17A and B, 39A and B, and 53A and B. They were refined as Ala. Residue 49A was refined as Gly. The deviation from ideality of the stereochemical parameters together with their target values is presented in Table 3. The avarage temperature factor for the final model is 22.2 Å^2. The structure contains 818 protein atoms for the two independent molecules and 125 water molecules. Comparisons of the two structures were carried out using least-squares minimization between the coordinate sets (*34*).

Assignments: ^{13}C NMR Spectra. The 1D ^{13}C spectra of the carbonyl region (Figure 1) show a remarkable resolution, and the variation from analogue to analogue is limited. Due to this similarity, the ^{13}C spectra are assigned based on the previous "full" assignment of WT BPTI (*22*) and supplementary information from the titration behavior of the ^{13}C chemical shifts of carbonyl carbons and on information obtained by the method of deuterium isotope effects (*21*). The two-bond and three-bond isotope effects were monitored in parallel with the decrease of the N*H* resonances. Observation of three-bond isotope effects is a very valuable tool, since only a few specific resonances show this feature (*35*). The chemical shifts and isotope effects are given in Table 1S (see Supporting Information). Deuterium isotope effects are normally monitored at pH 2.5. The increase in exchange rates for some of the less stable analogues make the number of measurable isotope effects slightly smaller. This feature can again be linked to NH exchange rates of Tables 1 and 2, and the absence of isotope effects can thus be used to confirm assignments. This is true for 3-58BPTI(K15R, R17A,R42S), and furthermore, in this particular case, the resemblance with that of 3-58BPTI(R17A,R42S) is so large that all resonances could be assigned unambiguously.

The titration shifts are investigated at three different pH values in the range from 2.5 to 1.5. Although very moderate chemical shift changes occur in the range from 2.5 to 1.5, the titratable side-chain carbonyl carbon resonances of the Glu and Asp residues and the C-terminal carbon could be assigned unambiguously. In the high-frequency part of the CO carbon shift range, the Glu and Asp resonances could be identified.

The comparison of the ^{13}C spectra of WT and 3-58BPTI confirms the CO suggested assignment of Arg-1 (*22*) and gives support to an assignment of the Pro-2 carbonyl carbon, Glu-7, Pro-8, and Arg-39 resonances of the WT protein. A comparison of the spectra of 3-58BPTI(R42S) with that of 3-58BPTI confirms the assignment of Arg-42 CO, and likewise can the assignments of the carbonyl resonances of Lys-15 and Arg-17 be deduced from comparison of relevant analogue spectra. The CO resonances of the replacing residues Ser-42, Ala-17, and Arg-15 have also been localized (Table 1S).

The assignments of the C-ξ of the six arginines of WT BPTI have not previously been reported. The HMBC spectrum of this region is very crowded (*22*). The spectra of the analogues show very few variations (Table 4), indicating that the resonances belonging to Arg-1 can be assigned to 157.8 ppm since the WT protein contains this residue and 3-58BPTI does not. By similar procedures it is possible to assign C-ξ resonances for Arg-42 [3-58BPTI-(R42S) vs 3-58BPTI] and Arg-17 [3-58BPTI(R17A,R42S) vs 3-58BPTI(R42S)]. The remaining resonances belonging to Arg-20, Arg-39, and Arg-53 could now be assigned based on the HMBC spectrum (Table 4).

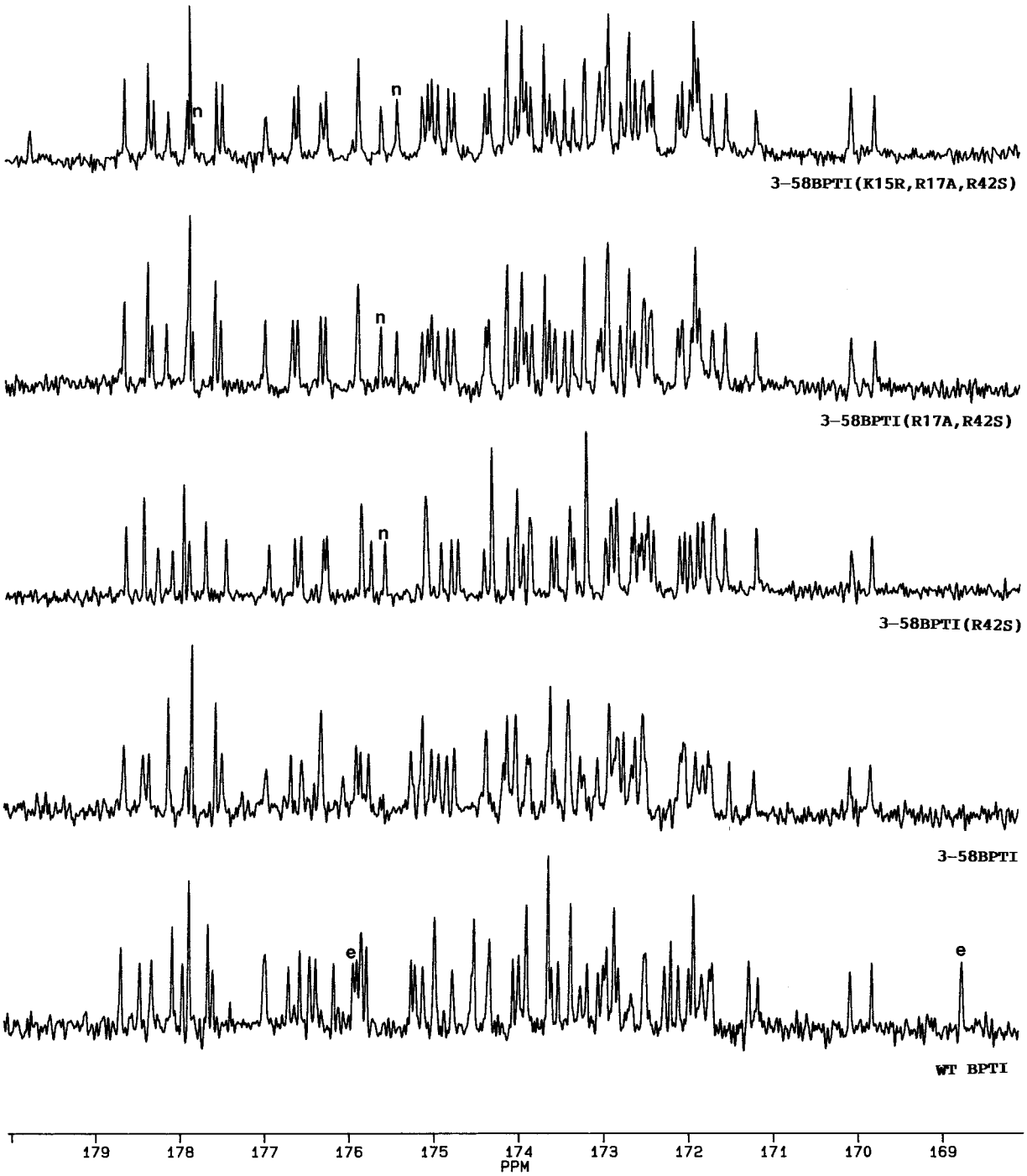

FIGURE 1: Carbonyl carbon resonances for WT BPTI (aprotinin) and 3-58BPTI analogues. pH 1.5 and temperature = 300 K. WT BPTI (aprotinin); 3-58BPTI; 3-58BPTI(R42S); 3-58BPTI(K15R,R17A,R42S); and 3-58BPTI(R17A,R42S). For assignments see Table 1S. *n* means resonance belonging to new residue. *e* means extra or external residue. These are residues 1 and 2 of WT BPTI.

RESULTS

^{13}C NMR. A comparison of the ^{13}C spectra of 3-58BPTI with that of WT BPTI revealed differences as shown in Tables 4 and 6 and illustrated in Figure 1. These differences are mostly but not exclusively located around resonances belonging to residues close to the two terminii. It is interesting to note the behavior of the broad resonance of Tyr-23 C-ξ in the ^{13}C spectrum of the WT protein, a resonance that becomes much sharper in 3-58BPTI and also in the derivatives thereof.

Table 4: Assignment of Arginine C-ϵ Resonances[a]

WT(aprotinin)	3-58BPTI	3-58BPTI-(R42S)	3-58BPTI-(K15R,R17A,-R4 2S)	assignment
157.8				Arg-1
157.8	157.8	157.8		Arg-17
157.65	157.65	157.65	157.65	Arg-20
158.0	158.0	158.0	158.0	Arg-39
157.7	157.7			Arg-42
157.92	157.92	157.92	157.92	Arg-53
			157.92	Arg-15

[a] Values in parts per million.

Table 5: Differences in ^{13}C Chemical Shifts of 3-58 BPTI Compared to WT BPTI (in parts per million)[a]

residue	C═O	C-α	C-β	others
Asp-3	3-5			C-γ (x)[b]
Phe-4	0.65	(x)[b]	(x)	C-δ 0.1
				C-ϵ 0.3
Cys-5	>0.5	(x) rc[d]		
Leu-6			(x)	C-γ 0.4
				C-δ 0.3
Glu-7				C-γ 0.3[c]
Phe-22	−0.1			C-γ 0.1
Tyr-23				C-γ 0.1
				C-ϵ 0.4
				C-ζ 0.3
Ala-25	0.05 rc		0.3 rc	
Ala-27	0.1			
Gly-28	0.1 rc			
Leu-29		(0.5) rc		C-γ 0.1
Phe-33				C-γ 0.1
Val-34	0.15			
Arg-42	0.09	0.2	0.4	
Asn-43			0.1	C-γ 0.05
Glu-49			(x)	
Glu-50				C-γ 0.25
Cys-51	(x) rc			
Met-52		0.2	0.2	C-ϵ 0.2 rc
				C-γ 0.2 rc
Arg-53	0.15			
Thr-54	0.15			C-γ 0.1
Cys-55	>0.2 rc			
Gly-56	>0.1	(x) rc		
Gly-57	>0.4	(x) rc		
Ala-58	0.6[d] rc	rc	0.3 rc	

[a] pH 2.5. Positive means to higher frequency in WT BPTI. [b] x means observed but small. [c] Much smaller at pH 1.5 (see Figure 1). [d] rc refers to ring current effets from Tyr-23 (see also Table 6).

A comparison of ^{13}C data for the two truncated analogues 3-58BPTI and 3-58BPTI(R42S) reveal very few changes and mainly around the substituted residue, Arg-42. The carbonyl resonances of Ala-40, Lys-41, Asn-43, and Asn-44 are shifted and so is the C-γ of Phe-4 and the carboxyl carbon of Glu-7. It is clear that this amino acid substitution primarily has an effect on the nearest neighbors, with the exceptions of two resonances, those of Glu-7 C-δ and Phe-4 C-γ (see Discussion). A comparison of the ^{13}C spectra of 3-58BPTI-(R42S) and 3-58BPTI(R17A,R42S) confirms this picture. Only the CO resonances of Ala-16, Ile-18, and to a lesser extent, Cys-14 are shifted.

The conservative replacement of Lys-15 with Arg-15 in 3-58BPTI(K15R,R17A,R42S) causes hardly any changes except for the resonance of residue 15, whereas the additional Arg-17 to Ala replacement causes a sizable shift of the carbonyl resonance of Ala-16.

X-ray. The structure of 3-58BPTI(K15R,R17A,R42S) has two molecules per asymmetric unit, called A and B. The backbone structure of these are quite similar as seen from Figures 2 and 3. The conformations of the side chains, especially that of Phe-4, are different in the two molecules. It is interesting to notice that no electron density could be asssigned to the side chain of Glu-7. A comparison of these structures with that of the WT BPTI reveals again only minor differences in the backbone (Figure 3). These differences are mainly found around the loop 24−28. A similar finding is reported for S-bridge variants (*36*). Side-chain differences between unit A and the WT BPTI are minor as can be inferred from a comparison of data of Figure 3.

Table 6: Calculated ^{13}C Ring Current Effects in WT and Differences in Ring Currents between This and 3-58BPTI(K15R,R17A,R42S) (in Brackets)[a]

residue	C═O	C-α	C-β	other
Asp-3	(0.15)[d]	(0.24)[d]	(0.14)	
Phe-4	0.24[b]			C-ϵ1 0.12(0.12)[d]
				C-ϵ2 (0.04)
Cys-5	0.25	0.13[b]	(−0.14)	
	(0.11)	(0.16)		
Pro-9	−0.28	−0.66	−1.33	C-γ −1.02 (0.11)[d]
	(0.08)[d]		(0.19)[d]	C-δ −0.63[d]
Tyr-10		0.29		
Gly-12	−0.19	−0.40		
Arg-20	−0.06	−0.16	−0.36	
	(0.14)	(0.11)	(0.07)	
Tyr-21	0.74[d]	0.63	0.10	
Phe-22		0.69		
Tyr-23		0.37		
Asn-24	−0.61[b]	−0.38[b,d]	−0.27	
	(−0.13)			
Ala-25		−0.09[b,d]		
Leu-29		(0.16)		
Gln-31			−0.27	
Thr-32	0.29		−0.28[b]	C-δ2 −0.73
Phe-33		0.39		
Tyr-35	−0.26		−0.25	
Gly-36	−0.48	−0.37		
Gly-37	−0.40	−0.53		
	(0.14)			
Arg-39	0.31	0.22	0.23	
Ala-40		(−0.10)[d]	−0.21	
Lys-41	−0.23			C-γ −0.46 (−0.11)[d]
				C-δ −0.48 (−0.12)[d]
				C-ϵ −0.56 (0.11)[d]
Arg-42	−0.65	−0.59	−0.85	C-γ[c] −0.45
	(−0.36)	(−0.33)	(−0.54)	C-δ[c] −0.25
Asn-43	0[b] (0.17)		(0.11)	C-γ 0.44
Asn-44	−0.17[b]	−0.03		C-γ −0.19 (0.31)
	(0.19)[d]	(0.25)[d]		
Phe-45	0.32	0.46		C-δ1 0.22
				C-ϵ1 0.28 (0.17)[d]
				C-ϵ2 0.17 (0.15)[d]
				C-ξ 0.33 (0.26)[d]
Ser-47	−0.46	−0.15[b]		
Ala-48	−0.32	−0.73	−0.57[b,d]	
Cys-51	−0.41[b]	−0.77[b]	−0.35[b]	
	(0.19)	(−0.18)	(−0.21)	
Thr-54	−0.20			
Cys-55	−0.78[d]	−0.51[d]	−0.51	
			(0.19)[d]	
Gly-56	−0.16	−0.34		
Gly-57		(0.11)		
Ala-58	(−0.26)[d]			

[a] Values for 3-58BPTI(K15R,R17A,R42S) are based on the a-subunit. Only values numerically larger than 0.1 ppm are usually included. [b] This carbon shows relatively large differences between data calculated for relaxed structures of WT and 4PTI (1). [c] These carbons do not exist in 3-58BPTI(K15R,R17A,R42S). [d] Values based on the b-subunit are slightly different.

Ring Currents. ^1H and ^{13}C ring current shifts are calculated for two BPTI structures. One was reported by Deisenhofer *et al.* (*1*), normally referred to as 4PTI, and the other made in this study for aprotinin at pH 9. The program applied is that of Williamson (*37*), and no special weight factors are used for the ^{13}C ring currents. Both WT BPTI X-ray structures were subject to a molecular mechanics energy minimization. The applied procedure included two steps of energy minimization (steepest descent and conjugated gradient, 200 steps each) using a distance-dependent dielectric constant. The crystal solvent molecules were

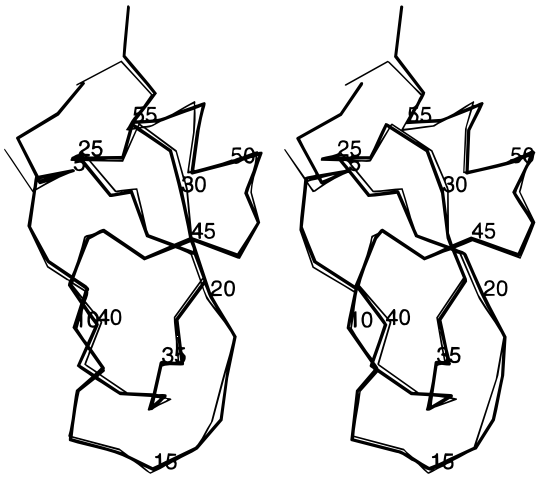

FIGURE 2: Comparison between WT BPTI (PDB filename, 4pti) and 3-58BPTI(K15R,R17A,R42S). The structure in thick line is WT BTPI.

included in the minimization. The mutant 3-58BPTI(K15R, R17A,R42S) was subjected to the same procedure. The ^{13}C ring currents of the relaxed structures were on the order of −1.35−0.78 ppm. The ring currents calculated for the two WT BPTI structures are similar within 0.2 ppm except for Arg-43 C′, Asn-44 C′, and Cys-51 C-α. A comparison of ring currents for WT and 3-58BPTI(K15A,R17A,R42S) (Table 6) reveals rather small differences <0.35 ppm except at residue Arg-42, which is replaced by serine in the derivative.

^{1}H NMR. Comparison of the ^{1}H spectrum of 3-58BPTI with that of the WT show some characteristic differences (Table 7). Similar, although smaller, differences were also seen for transaminated BPTI (*12*) and for N-terminally extended BPTIs (*7*). Easily monitored changes are those of Tyr-23 H-ϵ and Ala-58 H-β. It is characteristic that in case of Tyr-23 H-ϵ the changes increase in the series 4-BPTI < T-BPTI < 3-58BPTI, but not any further in the analogues of 3-58BPTI with additional substitutions.

A titration study monitoring the CH_3 chemical shift of Ala-58 vs pH in the range from 1.5 to 6 gave a pK_a value of the C-terminal carboxylic acid of 3.72.

NH Exchange Rates. NH exchange rates for selected protons of all analogues are measured as shown in Tables 1 and 2. These NH protons are among the slowest exchanging protons, with well-resolved peaks and characteristic chemical shifts. Chemical shift changes are minor for this group of protons in the specifically modified proteins, and the signals were easily identified by comparison with the WT BPTI spectrum. Conditions are chosen such that the exchange rates are on a suitable time scale, and data collected for all analogues can be compared with data for WT-BPTI, transaminated BPTI (*12*), and N-extended BPTI (*7*).

At both temperatures investigated, 45 and 58 °C, exchange rates increased for all protons in the order WT-BPTI < 3-58BPTI < 3-58BPTI(R42S) < 3-58BPTI(R17A,R42S) < 3-58BPTI(K15R,R17A,R42S) and follows the decrease in TTEP temperatures (Tables 1 and 2).

The six residues Gln31, Phe45, Met52, Phe22, Tyr23, and Tyr21 are covered by measurements with all four analogues at 45 °C. For these residues, exchange rates of 3-58BPTI are 10−50 times faster than for WT-BPTI, whereas exchange

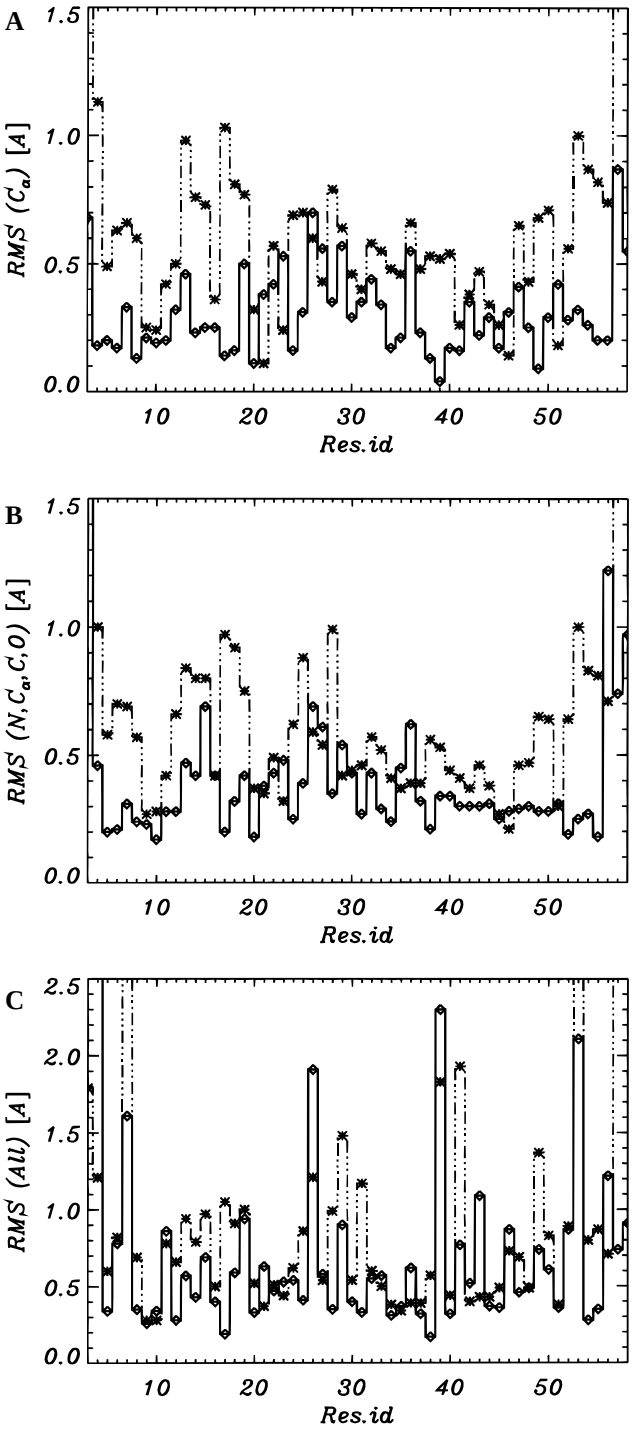

FIGURE 3: Rms differences (in angstroms) between α-carbons of WT BPTI (6PTI) (*3*) and 3-58BPTI(K15R,R17A,R42S) in angstroms. (A) A-unit−B-unit in full lines and A-unit of 3-58BPTI-(K15R,R17A,R42S)−WT BPTI in dot−dashed lines. (B) RMS differences between N,C-α,C,O atoms of A-unit−B-unit of 3-58BPTI(K15R,R17A,R42S) in full lines and between WT BPTI and A unit in dot−dashed lines. (C) RMS differences between all atoms of A-unit−B-unit in full lines and between WT BPTI and A-unit in dot−dashed lines.

rates of 3-58BPTI(R42S) are 30−330 times faster. Those of 3-58BPTI(R17A,R42S) are 250−1900 times faster, and those of 3-58BPTI(K15R,R17A,R42S) are 400−2200 times faster. Within the series of protons for WT-BPTI, the variation in exchange rates is large at this temperature. The fastest and the slowest rates differ by a factor 8, and if Tyr-35 and Phe-33 are withdrawn, the difference is 50-fold. For

Table 7: ^{1}H Chemical Shift Differences of between Modified BPTIs and WT BPTI (in ppm)

residue	3-58 BPTI	4-BPTI
Asp−3 H-β	0.05	0.02
Phe−4 H-δ	0.03	0.02
Leu−6 H-δ	0.03	0.01
Tyr−23 H-ϵ	0.06	0.04
NH	0.02	0.04
Ala−27 H-β	0.02	0.01
Ala−40 H-β	0.02	0.01
Met−52 H-ϵ	0.01	0.01
Ala−58 H-β	0.07	0.05

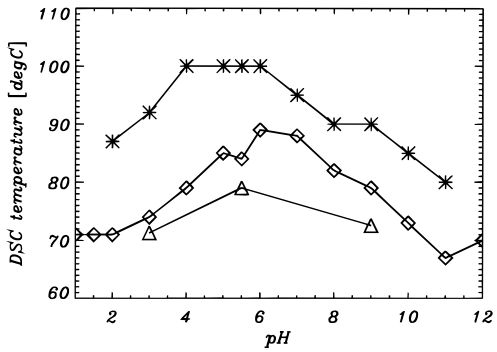

FIGURE 4: Plot of TTEP temperatures (from DSC experiment) vs pH for BPTI(aprotinin) and analogues. BPTI (aprotinin) (*), 3-58BPTI (◇), 3-58BPTI(R42S) (△).

the analogues, exchange rates are very uniform, and variations by only a factor of 2−3 are seen.

At 58 °C, a comparison is relevant for the six slowest exchanging protons: Arg-20, Tyr-21, Phe-22, Tyr-23, Gln-31, and Phe-45. Exchange rates increase 80−160 times from WT-BPTI to 3-58BPTI and 300−670 times from WT-BPTI to 3-58BPTI(R42S).

The change in unfolding free energy between WT-BPTI and the modified proteins can be estimated as $\Delta G_U = RT\ln(k^{mut}/k^{WT})$ (*38*). When ΔG_U is calculated for single protons, Tyr-23 NH gives the largest value at both temperatures for all four analogues. The estimates for Tyr-23 of 3-58BPTI are 2.5 kcal/mol using the 45 °C data and 3.3 kcal/mol using the 58 °C data. The energy for 3-58BPTI(R42S) is changed by 3.7 or 4.3 kcal/mol, depending on which data set is used. Estimates from the 45 °C data are 4.8 kcal/mol for 3-58BPTIR(R17A,R42S) and 4.9 kcal/mol for 3-58BPTI-(K15R,R17A,R42S).

Differential Scanning Calorimetry. The high stability of BPTI makes possible an investigation of the thermal unfolding over a broad pH range. DSC measurements of WT BPTI, 3-58BPTI, and of 3-58BPTI(R42S) are shown in Figure 4. The curves are all bell shaped with clearly different pH maxima, 5 and 6.25, respectively. The plateau seen for WT BPTI between pH 8 and 9 coincides with the plateau found by Roder *et al.* (*26*) for NH exchange rates.

Temperatures at the top of the endothermic peak (TTEP) measured at pH 5.5 are given in Table 1.

DISCUSSION

^{13}C NMR. The comparison of ^{13}C chemical shifts for WT BPTI and 3-58BPTI show differences around the terminii. In truncated derivatives, these changes are partly due to loss of the interaction between the terminii and partly due to the positive charge of the new N-terminus. This charge at Asp-3 of the truncated derivatives affects the chemical shifts of the carbonyl carbons of Asp-3, Phe-4, and Cys-5 strongly (Table 5). Removal of the salt bridge is indicated by a change in the pK_a values of Ala-58 toward a higher and more normal value, 3.72. This change is also seen in the chemical shift of the COO^- carbon resonance of Ala-58 of 3-58BPTI and the analogues thereof, as compared to the chemical shift change of WT BPTI. A change in the pK_a value was also found for T-BPTI (*12*), for des(Ala-16,Arg-17)BPTI (*13*) and for 4-BPTI (*7*). The removal of residues 1 and 2 creates an easier access to the core of the protein as seen in Figure 5.

As a result of N-terminal truncation, two conspicuous observations are made concerning the Tyr-23. First, the H-ϵ is shifted in 3-58BPTI and the C-ξ resonance is narrowing in 3-58BPTI. Second, the resonances in the vicinity of Tyr-23 are shifted from the WT BPTI to 3-58BPTI. We ascribe these changes (marked with rc in Table 5) to an increased mobility of the Tyr-23 ring in 3-58BPTI and possibly a change in the average position, which in turn causes a change in the ring current effects at the neighboring atoms.

The chemical shift variations observed between 3-58BPTI and 3-58BPTI(R42S), between 3-58BPTI(R42S) and 3-58BPTI(R17A,R42S), and between the latter and 3-58BPTI-(K15R,R17A,R42S) can be ascribed to local changes in chemical shifts due specific amino acid replacements. These substitutions give an idea about the effects of an amino acid on chemical shifts of neighboring carbonyl carbons. Replacement of Lys-15 for Arg had hardly any effect, of Arg for Ala, the effect at the neighboring carbonyl carbons is 0.45 ppm and 0.18, whereas of Ser for Arg, the effect is much more severe (Table 1S). However, this could be related to the removal of the side chains of Arg-42. This is also seen in the chemical shift difference found for Glu-7 Cγ when comparing 3-58BPTI and 3-58BPTI(R42S). For the WT BPTI, the side chain of Arg-42 seems to be in the all trans position as evidenced from the very weak resonances due to C-ξ, Hδ in the HMBC spectrum (*22*). This is a result of the involved three bond coupling constants being both of "gauche" type and hence small. A similar picture is seen for Arg-20, whose side chain forms a hydrogen bond to Asn-44Cγ. A third indicator of a more rigid structure around the C-δ, C-ϵ bond is the nonequivalence of the two H-δ protons of these residues.

From the very small chemical shift differences of the C-ξ carbons of the arginines, it is concluded that these residues are not responding to salt bridge formation.

The ^{13}C and ^{1}H chemical shift studies can therefore be summarized as follows: the interaction between the terminals observed in WT BPTI is clearly absent in 3-58BPTI and the other truncated analogues of this study. This is in agreement with previous findings with T-BPTI and the extended BPTI derivatives such as 4-BPTI. Apart from that, changes in structure are only minor as also indicated by the X-ray diffraction study of 3-58BPTI(K15R,R17A,R42S).

Specific amino acid substitutions, although resulting in very small changes in structure can clearly be pinpointed by ^{13}C NMR. Salt bridges can also be identified by such replacements, as indicated by changes in carboxyl carbon chemical shifts of the residues involved.

NH Exchange. NH exchange data for the truncated and modified proteins at the present conditions point toward an

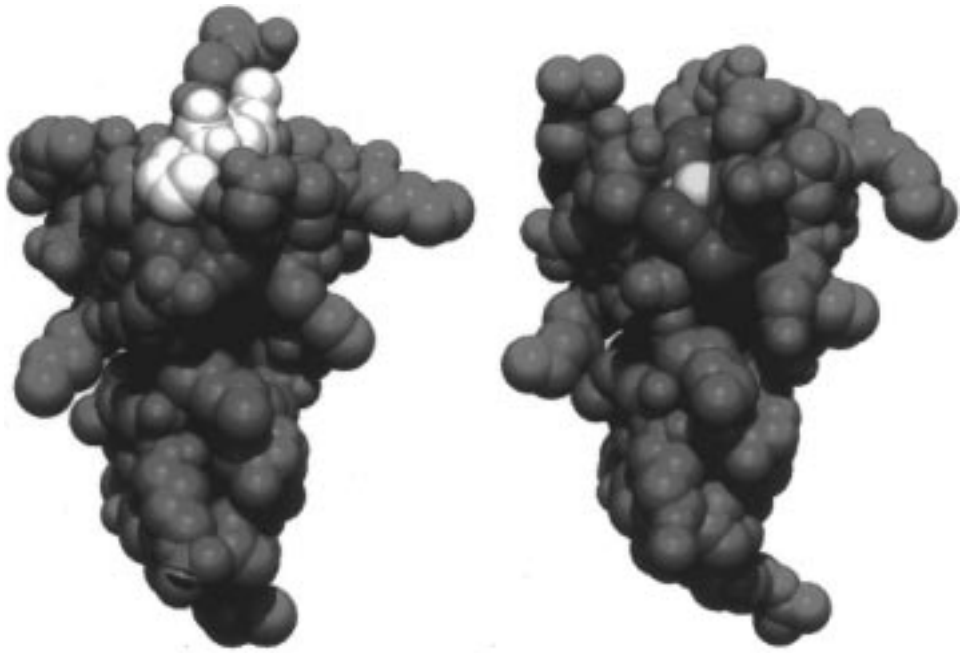

FIGURE 5: Space filling model of 3-58BPTI(K15R,R17A,R42S). The two first residues of WT BPTI are marked with white. Phe-4, Cys-5 and Cys-55 are marked in blue, except for the S−S bridge, which is marked in yellow. The more open structure for 3-58BPTI(K15R,-R17A,R42S) is seen by the appearance of the disulfide sulfurs of Cys-55 (marked with yellow).

increased contribution to the exchange from thermal global unfolding. Rates for the slowest exhanging protons is strongly increased even at 45 °C and becomes uniform and similar to the rates for the faster exchanging NH protons such as those of, e.g., Tyr-35 and Ile-18. Structural changes are only reflected as weak trends, such as the finding that the rate of Tyr-23 NH is generally influenced the most. It is interesting to note that des(Ala-16,Arg-17)BPTI gives rise to quite a different picture (*39*).

Some chemical shifts, exchange rates, and TTEP temperature were seen to develop in parallel for the extended BPTIs and T-BPTI. This pattern also applies to 3-58BPTI, but not to the derivatives with further replacements. The resonances that show chemical shifts changes belong to nuclei in Tyr-23 or in the vicinity of this residue. For 3-58BPTI, the changes in chemical shifts, in exchange rates, and in stability are all clearly caused by the change at the terminii leading to a more open structure (Figure 5) as also seen by the higher mobility of the Tyr-23 ring. The largest destabilization of the molecule comes from the removal of the two N-terminal residues. It is also significant that the leveling effect of 3-58BPTI(R42S) at 48 °C and pH 1 is very similar to that of WT-BPTI at 60 °C and pH 1.

The further increase in N*H* exchange rates and decrease in stability is related to changes caused by specific amino acid substitutions of the 3-58BPTI derivatives. For 3-58BPTI-(R42S), this change in stability can possibly fully or in part be related to the removal of an interaction between Glu-7 COOH and Arg-42 NH-ξ, although, its existence is tentative since the structure of the side chain varies as determined by existing differences between X-ray studies (*3, 40*).

Estimates for changes in unfolding free energy is in fair agreement with the TTEP results taking into account that different buffers are used. A comparison of $\Delta\Delta G$ for 3-58BPTI at different pHs reveal that $\Delta\Delta G$ is larger at pH 6.5 than at pH 1. A similar result is found for 3-58BPTI-(R42S). These results point to the importance of pH in such measurements and can be understood as a result of the fact that the stability of the WT BPTI and analogues varies differently as a function of pH (Figure 4).

CONCLUSIONS

The differences between the X-ray structures of the WT and 3-58BPTI(K15R,R17A,R42S) are rather small (Figures 2 and 3) concerning the backbone. The differences are to some extent obscured by the existence of two molecules in the asymmetric unit (Figure 3). However, as seen in Figure 5, the lack of the two N-terminal residues combined with the consequent lack of a salt bridge between the two terminals leads for the truncated analogues to a structure open at one end (Figure 5). Studies of NH exchange rates show a much increased exchange rate for the truncated analogues.

^{13}C NMR studies of proteins and in particular of the carbonyl region is shown to be a sensitive and a convenient method for scanning of analogues for structural changes.

Resonances of the carbonyl region are well suited for this purpose because they are relatively easy to assign and measure accurately. Further, these resonances are expected to stay sharp for even very large proteins.

The carboxyl resonances of side chains are shown to be potentially valuable as monitors of the existence of salt bridges.

The differences in chemical shifts observed between WT BPTI and the truncated analogues are divided into two groups, those caused by N-terminal modifications that induce structural changes and those caused by single amino acid substitutions that induce local perturbations not related to a general structural change. Changes in chemical shifts related to a change in the conformation of the terminii involve charge effects from the N-terminal NH_3^+ group and ring current effects caused by changes in the mobility and conformation of the aromatic ring primarily of Tyr-23.

ACKNOWLEDGMENT

The authors wish to thank Dr. M. P. Williamson for the modification and use of the ring current program.

SUPPORTING INFORMATION AVAILABLE

One table giving ^{13}C chemical shifts together with information about titration behavior and presence of two- and three-bond isotope effects for the carbonyl carbons of of the analogues at pH 1.5 is available (6 pages). Ordering information is given on any current masthead page.

REFERENCES

1. Deisenhofer, J., and Steigeman, W. (1975) *Acta Crystallogr. B31*, 238−50.
2. Wlodawer, A., Walter. J., Huber, H., and Sjølin, L. (1984) *J. Mol. Biol 180*, 301−329.
3. Wlodawer, A., Deisenhofer, J., and Huber, H. (1987) *J. Mol. Biol. 193*, 145−156.
4. Housset, D., Kim, K.-S., Fuchs, J., Woodward, C.; Wlodawer, A. (1991) *J. Mol. Biol. 220*, 757−770.
5. Danishefsky, A. T., Housset, D., Kim, K.-S., Tao, F., Fuchs, J., Woodward, C., and Wlodawer, A. (1993) *Protein Sci. 2*, 577−587.
6. Berndt, K. D., Gunthert, P., Orbons, L. P. M., and Wüthrich, K. (1992) *J. Mol. Biol. 227*, 757−775.
7. Lauritzen, C., Skovgaard, O., Hansen, P. E., and Tüchsen, E., (1992) *Int. J. Biol. Macromol. 14*, 326−332.
8. Otting, G., Liepinsch, E., and Wüthrich, K. (1993) *Biochemistry 32*, 3571−3582.
9. Goldenberg, D. P., and Creighton, T. E. (1984) *J. Mol. Biol. 179*, 527−545.
10. Eigenbrot, C., Randal, M., and Kossiakov, A. A. (1990) *Protein Eng. 3*, 591−598.
11. van Mierlo, C. P. M., Darby, N. J., Neuhaus, D., and Creighton, T. E. (1991) *J. Mol. Biol. 222*, 353−371.
12. Brown, L. R., de Marco, A., Richarz, R., Wagner, G., and Wüthrich, K. (1978) *Eur. J. Biochem. 88*, 87−95.
13. Siekmann, J.; Wenzel, R. R., Schröder, W., Schutt, H., Truscheit, E., Arens, A., Raenbusch, E., Chazin, W. J., Wüthrich, K., Tao, F., Fuchs, J. A., and Woodward, C. (1993) in *Techniques in Protein Chemistry (IV)* (Anglettei, R., Ed.) p 512−520, Academic Press. San Diego.
14. Lauritzen, C., Tüchsen, E., Hansen, P. E., and Skovgaard, O. (1991) *Protein Expression Purif. 2*, 372−378.
15. Norris, K., Norris, F., Bjørn, S. E., Diers, I.; Petersen, L. C. (1990) *Biol. Chem. Hoppe-Seyler 371 (suppl.)*, 37−42.
16. Fersht, A., and Serrano, L. (1993) *Curr. Opin. Struct. Biol. 3*, 75−83.
17. Dao-pin, S., Nicholson, H., and Matthews, B. W. (1991) *Biochemistry 30*, 7142−7152.
18. Bax, A. (1989) *Annu. Rev. Biochem. 58*, 223−256.
19. Bodenhausen, G., and Ruben, D. J. (1980) *Chem. Phys. Lett. 69*, 185−189.
20. Bax, A., and Summers, M. F. (1986) *J. Am. Chem. Soc. 107*, 2821−2822.
21. Tüchsen, E., and Hansen, P. E. (1988) *Biochemistry 27*, 8568−8576.
22. Hansen, P. E. (1991) *Biochemistry 30*, 10457−10466.
23. Blanchard, L., Hunter, C. N., and Williamson, M. P. (1997) *J. Biomol. NMR 9*, 389−395.
24. Horovitz, A., Serrano, L., Avron, B., Bycroft, M., and Fersht, A. R. (1990) *J. Mol. Biol. 216*, 1031−1044.
25. Hilton, B. D., and Woodward, C. K. (1979) *Biochemistry 18*, 5834−5841.
26. Roder, H., Wagner, G., and Wüthrich, K. (1985) *Biochemistry 24*, 7396−7407.
27. Davies, D. R., and Segal, D. M. (1971) *Method Enzymol. 22*, 266−269.
28. Matthews, B. W. (1968) *J. Mol. Biol. 33*, 491−497.
29. Hendrix and Lentfor, unpublished results.
30. Leslie, A. G. W., Brick, P., and Wonacott, A. J. (1986) *CP4 Newslett. 18*, 33−39.
31. Hendrickson, W. A., and Konnert, J. H. (1980) in Biomolecular Structure, Function and Conformation and Evolution (Srinivisan, R., Ed.) Vol. 1, pp 43−57, Pergamon, Oxford.
32. Baker, E. N., and Dodson, E. J. (1980) *Acta Crystallogr. A36*, 559−572.
33. Jones, T. A. (1978) *J. Appl. Crystallogr. 11*, 268−272.
34. Kabsch, W. (1978) *Acta Crystallogr. A32*, 922−923.
35. Tüchsen, E., and Hansen, P. E. (1991) *Int. J. Biol. Macromol. 13*, 1−9.
36. Kossiakov, A. A., Randal, M., Guenot, J., and Eigenbrot, C. (1992) *Proteins: Struct., Funct., Genet. 14*, 65−74.
37. Williamson, M. P. Private communication.
38. Kim, K. S., Tao, F., Fuchs, J., Danishefsky, A. T., Housset, D., Wlodawer, A., and Woodward, C. (1993) *Protein Sci. 2*, 588−596.
39. Wagner, B., Tschesche, H., and Wüthrich, K., (1979) *Eur. J. Biochem. 95*, 239−248.
40. Schiffer, A. A., Huber, R., Wüthrich, K., and van Gunsteren, W. F. (1994) *J. Mol. Biol. 241*, 588−599.
41. Wagner, G., and Wüthrich, K. (1982) *J. Mol. Biol. 160*, 343−361.

BI972282U